Transient Inclusion Evolution During Modification of Alumina Inclusions by Calcium in Liquid Steel: Part II. Results and Discussion

N. VERMA, PETRUS C. PISTORIUS, RICHARD J. FRUEHAN, MICHAEL POTTER, MINNA LIND, and SCOTT R. STORY

The formation of intermediate reaction products after calcium addition to aluminum-killed steel was studied. Steel samples were taken from laboratory and industrial heats before and at various times after calcium treatment. Inclusions were characterized by automated and manual scanning electron microscopy and X-ray microanalysis of polished cross sections and inclusions extracted by dissolution of the steel. Industrial and laboratory melts containing more than 40 parts per million (by mass) of dissolved sulfur showed calcium sulfide as the main reaction product after calcium injection, with calcium aluminates appearing later. It is proposed that the calcium aluminates are formed by reaction between the calcium sulfide and the alumina. A laboratory heat containing 7 parts per million of sulfur showed calcium oxide as the main initial calcium reaction product. A simple mechanism is proposed for the modification of alumina inclusions by calcium, considering transient CaO and CaS formation.

DOI: 10.1007/s11663-011-9517-2

I. INTRODUCTION

As discussed in Part I, this research tested the hypothesis that, upon calcium injection into liquid steel, CaS forms and plays a central role in subsequent modification of alumina inclusions. This suggestion is based on previous research that demonstrated CaS to be an intermediate reaction product.[1–4] The reaction responsible for modification of alumina is hence proposed to be as follows:

$$3CaS + Al_2O_3 \rightarrow 3(CaO) + 2[Al] + 3[S] \qquad [1]$$

If this mechanism held, then the inclusions would be a mixture of CaS and Al_2O_3 immediately after calcium injection, converting to calcium aluminates by reaction [1]. In reaction [1], [Al] and [S] represent the species dissolved in Fe and (CaO) indicates CaO in the inclusion. The proposed reaction path is illustrated in Figure 1. If the proposed mechanism held, the inclusion compositions would lie along the CaS-Al_2O_3 join after calcium injection; after subsequent reaction, Al and S would be returned to the steel melt by reaction [1], causing the inclusion compositions to follow the arrows in Figure 1. The molar ratio of Ca/Al in the non-CaS portion of the inclusion (indicated by $[Ca/Al]_{mod}$ in the figure, and as explained in Part I) would be increased by the reaction. Successful modification would require the resulting inclusion composition to lie within the shaded region in Figure 1; this shaded region is the range of compositions that are at least 50 pct liquid, at 1823 K (1550 °C) (as calculated with FactSage 6.2 [ThermFact Inc., Montreal, Canada] using the FSstel and FToxid databases[5]).

To test this possibility, aluminum-killed heats containing 7 ppm to 100 ppm sulfur were calcium treated in the laboratory, taking steel samples before and at various times after calcium treatment. In all cases, as demonstrated previously in Part I, the sulfur content of the steel was sufficiently low to ensure that solid CaS was not stable in contact with alumina or $CaAl_2O_4$-saturated liquid calcium aluminate inclusions. Several samples from industrial heats were also analyzed, and a typical example is given in this paper. For the industrial sample, the heat size was 200 metric tons, and the amount of calcium silicide injected (for calcium treatment) was 170 kg. The steel composition of the industrial heat is reported in Table I.

II. RESULTS AND DISCUSSION

A. *Laboratory Heats*

1. *Inclusion compositions*

Table II gives the bulk analyses of the heats after calcium treatment (as discussed in Part I, Al_2O_3 inclusions were present after aluminum deoxidation).

N. VERMA, Ph.D. Candidate, and PETRUS C. PISTORIUS and RICHARD J. FRUEHAN, Professors, are with the Department of Materials Science and Engineering, Center for Iron and Steelmaking Research, Carnegie Mellon University, Pittsburgh, PA 15213. Contact e-mail: pcp@andrew.cmu.edu MICHAEL POTTER, Senior Scientist, is with the RJ Lee Group, Monroeville, PA 15146. MINNA LIND, formerly Visiting Researcher, Carnegie Mellon University, is now Postdoctoral Researcher with Aalto University, FI-00076 Aalto, Finland. SCOTT R. STORY, Research Consultant, is with the Department of Process Technology—Steelmaking and Casting, United States Steel Corporation Research and Technology Center, Munhall, PA 15120.

Manuscript submitted February 25, 2011.
Article published online April 22, 2011.

Number-averaged inclusion compositions from automated scanning electron microscope energy-dispersive X-ray analysis (EDX) microanalyses (ASCAT) are reported in Table III; the inclusions were mixtures of the components Al_2O_3, CaO, and CaS, and the reported compositions were normalized to 100 pct with respect to Al, S, and Ca (Mg levels in these inclusions were low, generally below the cut-off of 2 pct). In most cases, the inclusions showed the maximum sulfur content after calcium treatment, with the sulfur content of the inclusion decreasing with time. This was the case even for heat A, which contained only 7 ppm sulfur (although the inclusions detected in the sample taken 30 seconds after calcium treatment of this heat had a low sulfur content, the sulfur content was considerably higher in the inclusions in sample taken after 2 minutes and then lower in the sample taken after 4 minutes; Table III).

Given the high sulfur content of the inclusions in the samples collected 2 minutes after calcium treatment, most of the calcium detected in the inclusions was present as CaS (except for heat A) and a smaller fraction as calcium oxide. These inclusions were poorly modified, with a low modified Ca/Al ratio. With increased time, the average sulfur content of the inclusions decreased (consistent with occurrence of reaction [1]), and the modified Ca/Al ratio increased: from 0.19 (2 minutes) to 0.29 (4 minutes) for heat C and from 0.16 (2 minutes) to 0.25 (4 minutes) for heat D. This shift is also illustrated by the distribution of inclusion compositions given in Figure 2: With time, the distribution of compositions shifted from being centered on the CaS-Al_2O_3 join to lying below that join at lower sulfur levels. This is as expected for the mechanism illustrated in Figure 1.

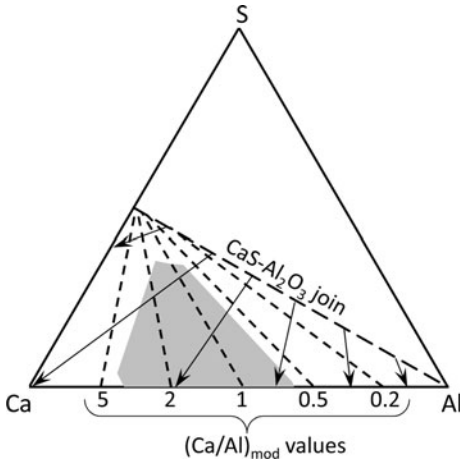

Fig. 1—Changes in inclusion compositions, for the proposed reaction between CaS and Al_2O_3 (showing the Al_2O_3-CaO-CaS inclusion compositions on a ternary diagram of mole fractions of Ca, S and Al). The CaS-Al_2O_3 join represents the inclusion compositions immediately after calcium treatment and arrows indicate the change in composition of inclusions as CaS and Al_2O_3 react.

Because of the resolution limits of backscattered electron imaging and EDX microanalysis, inclusions smaller than 1 μm in apparent diameter were not analyzed by ASCAT. As a result, not all inclusions in the steel were detected and analyzed. This is shown by the size distribution of detected inclusions (Figure 3), which seems to be truncated below 1 μm, and by the calculated Ca and O content of the detected inclusions, as fractions of the total steel mass (Table IV). The Ca and O contents were calculated by taking the area fraction to be equal to the volume fraction of inclusions,[6] finding the mass fraction of detected inclusions by assuming an average density of 3.5 g/cm^3 for the inclusions and 7.9 g/cm^3 for the steel, and calculating the Ca, O, S and Al mass percentages in the inclusions from stoichiometry. (The density of alumina is 4 g/cm^3, that of calcium aluminates varies from 2.9 g/cm^3 to 3.8 g/cm^3, and that of CaS is 2.6 g/cm^3.[7,8])

Although there is uncertainty regarding the concentration of dissolved calcium in the steel, it is estimated to be a few parts per million at most,[9] as is the concentration of dissolved oxygen in aluminum-killed steel.[10] Hence, most of the total Ca and O content of the steel (typically tens of parts per million) is present as inclusions, and a comparison of Ca and O detected in inclusions with their total contents allows an estimate of the extent to which some inclusions were not detected. As Table IV illustrates, the calcium contents indicate that approximately one third to one half of the inclusions were detected in samples taken 2 minutes after calcium treatment, with the oxygen contents indicating slightly smaller fractions. The fraction of inclusions detected was lowest for the low-sulfur heat (A), indicating a greater proportion of small inclusions in this heat.

Despite the uncertainty arising from nondetection of a large proportion of inclusions in the lowest-sulfur heat (heat A), it is evident from the distribution of (detected) inclusion compositions that the reaction mechanism was different for this heat (Figure 4). In the sample taken 30 seconds after calcium treatment, the detected inclusions were CaO and (unreacted) Al_2O_3. If it is the case

Table II. Bulk Chemical Analyses of Samples Collected 2 Minutes After Calcium Treatment for Different Laboratory Heats; Analyses Are in ppm by Mass

Heat	Al	Ca	O	S
A	1000	29	30	7
B	700	21	43	40
C	700	20	45	45
D	530	<20	47	100

Table I. Composition of Industrial Heat (Sample from Caster Mold); Mass Percentages

C	Mn	P	S	Si	Al	N	Ti	Cb	V	Ca
0.06	1.037	0.01	0.005	0.21	0.041	0.005	0.02	0.04	0.001	0.001

Table III. Average Composition of Inclusions (ASCAT Analyses) and Total Area of Detected Inclusions in Samples Collected at Various Times After Calcium Treatment from Different Laboratory Heats

Heat (S in ppm)	Samples	Average Inclusion Compositions			Area Fraction of Inclusions (ppm)
		Al (at. pct)	S (at. pct)	Ca (at. pct)	
A (7)	0.5 min after Ca	36	1	63	40
	2 min after Ca	12	14	74	50
	4 min after Ca	32	8	60	160
B (40)	0.5 min after Ca	48	20	32	20
	2 min after Ca	52	18	30	120
C (45)	Before Ca	100	0	0	40
	2 min after Ca	57	17	26	75
	4 min after Ca	68	7	25	125
D (100)	Before Ca	100	0	0	160
	2 min after Ca	63	14	23	90
	4 min after Ca	75	4	21	220

that most calcium is present in the steel in reacted form, then much of the calcium—at least 29 ppm based on the bulk analysis of the sample taken 2 minutes after calcium treatment—must have been present as calcium oxide, because reaction of all of the sulfur in the steel—7 ppm—could only account for 9 ppm of reacted calcium. Aluminum-killed steel typically contains around 4 ppm (by mass) of dissolved oxygen, which can react with 10 ppm calcium, and more oxygen can be released by dissociation of alumina.

With time, some CaS formed in the low-sulfur heat (heat A) by reaction of CaO with dissolved sulfur (or previously formed CaS became detectable by agglomeration of smaller CaS particles), as shown by the distribution of inclusions detected in the sample taken 2 minutes after calcium treatment (Figure 4). A significant proportion of calcium aluminate inclusions was detected only in the sample taken 4 minutes after calcium treatment (Figure 4). Although the reaction path of calcium was different in the lowest sulfur heat, the results do support the suggestion that calcium modification involves little or no direct reaction between calcium and alumina, but rather the formation of calcium reaction intermediates—CaS in higher sulfur heats and CaO in the lowest sulfur heat.

2. *Scanning electron microscopy of individual inclusions*

Scanning electron microscopy (of inclusions revealed on polished cross-sections, and others extracted by bromine-methanol) supported the roles of CaS and CaO as reaction intermediates. Inclusions in samples taken within 2 minutes of calcium addition to the higher sulfur heats (B, C, and D) commonly had a dual-phased morphology of CaS adhering to unmodified Al_2O_3; see Figure 5 for an example. This finding suggests that CaS nucleated heterogeneously on alumina; as also shown by the distribution of inclusion compositions (Figure 2), CaS was associated with alumina in almost all cases, rather than being detected as isolated CaS-only inclusions.

In samples taken later (4 minutes after Ca addition), the inclusions showed clear evidence of CaS having reacted with alumina, with Ca and Al (and O) present in the same region. As shown in Figure 6, a CaS ring was often observed around the inclusions (as discussed in Part I, this ring likely formed during solidification of the steel sample). The dual-phased CaS-containing inclusions were no longer observed. In many cases, voids were observed around the calcium-treated inclusions (Figure 7); the voids likely resulted from solidification shrinkage at the interdendritic positions to which the inclusions were pushed by the dendrites during solidification of the sample (it is feasible for the inclusions to have been pushed by the dendrites because the inclusion diameters were comparable with the interdendritic spacing[11]).

The extracted inclusions in Figure 8 exemplify the reaction path for inclusions in the higher sulfur heats (B, C, and D): After deoxidation of steel, clustered alumina inclusions formed. Immediately after calcium treatment, CaS was observed as an intermediate reaction product adhering to unmodified alumina. As time progressed, the inclusion morphology changed to spherical calcium aluminates through the reaction of CaS with alumina.

Figures 9 through 11 illustrate the evolution in composition of inclusions in the low-sulfur heat. Inclusions in the sample collected 30 seconds after calcium treatment of heat A (7 ppm S) were mostly CaO, small, and irregular in shape. In some cases, CaS was also found attached to CaO inclusions (Figure 9). In the sample collected 2 minutes after calcium treatment (Figure 10), the CaS content increased and CaO decreased, in line with the change in composition distribution (Figure 4). Some cases of CaS adhering to unmodified or partially modified alumina inclusions were also observed, similar to the morphology in the higher S heats. The sample collected 4 minutes after calcium treatment contained mostly inclusions, which were fully modified to liquid and with a low CaS content (Figure 11; compare with Figure 4(c)). In some instances, a partial CaS ring around the inclusions was observed.

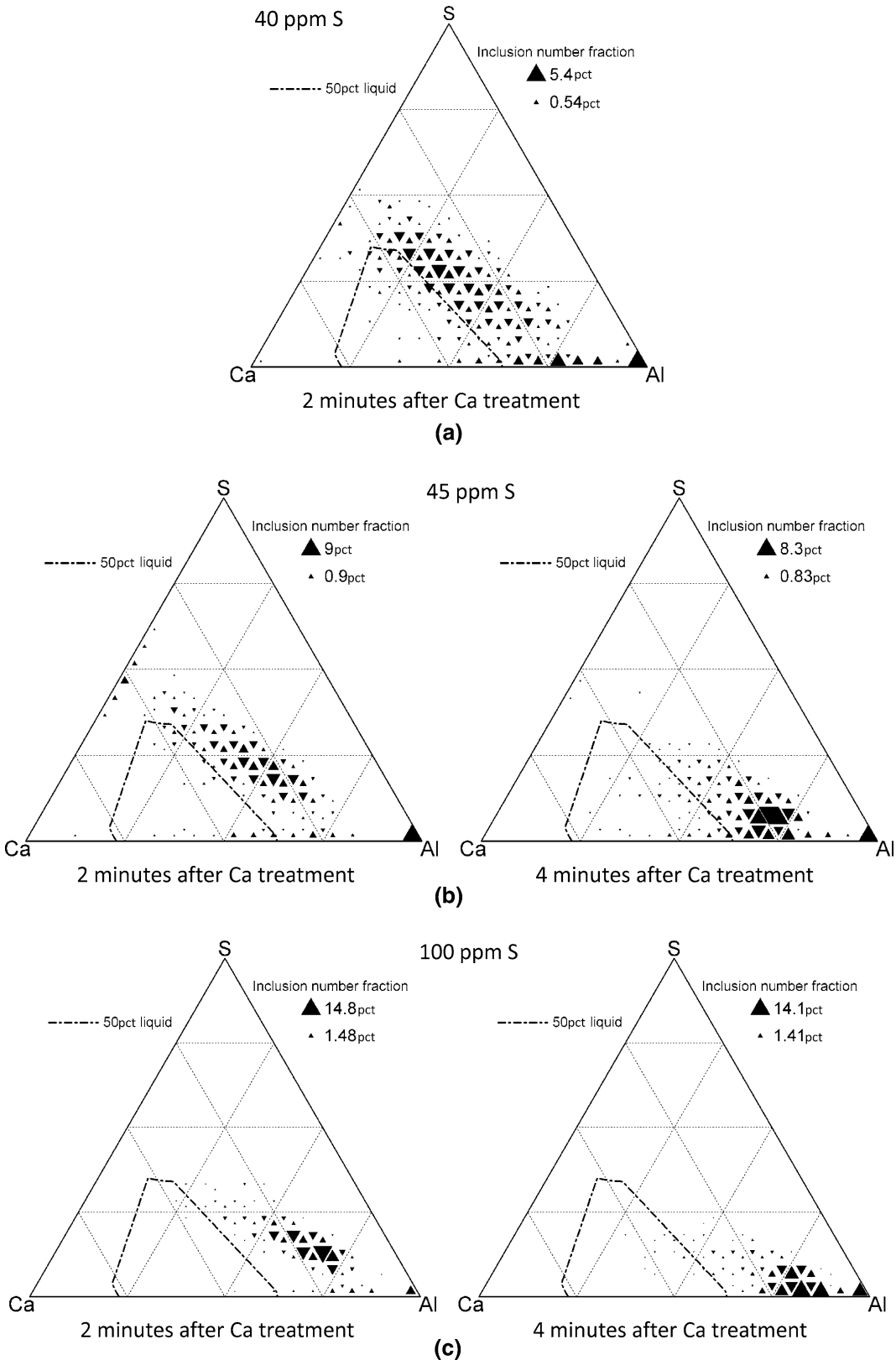

Fig. 2—Distributions of inclusion compositions (on ternary Ca-Al-S diagram; mole fractions), shown as proportional symbol plots. (*a*) Inclusions in heat B (40 ppm S, approximately 850 inclusions). (*b*) Inclusions in heat C (45 ppm S, approximately 750 inclusions each). (*c*) Inclusions in heat D (100 ppm S, approximately 900 inclusions each).

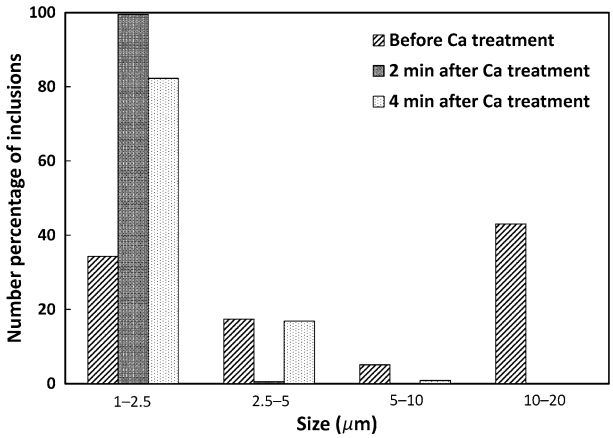

Fig. 3—Typical distribution of apparent diameters of inclusions detected (by ASCAT) on polished cross sections through samples taken at different times; heat D (100 ppm S).

Table IV. Ca, O, and S Content in Detected Inclusions, Expressed as ppm by Mass of the Steel, Calculated from the Average Compositions and Area Fractions Given in Table III; the Analyzed Steel Compositions from Table II are Repeated Here for Comparison

		Detected Inclusions (ppm)			Steel Bulk Analysis (ppm)		
Heat	Sample	Ca	O	S	Ca_{tot}	O_{tot}	S_{tot}
A	0.5 min after Ca	8	6	0			
	2 min after Ca	13	6	2	29	30	7
	4 min after Ca	33	22	4			
B	0.5 min after Ca	2	3	1			
	2 min after Ca	14	17	7	21	43	40
C	Before Ca	0	8	0			
	2 min after Ca	7	11	4	20	45	45
	4 min after Ca	11	21	2			
D	Before Ca	0	38	0			
	2 min after Ca	8	14	4	<20	47	100
	4 min after Ca	16	40	2			

B. *Industrial Samples (S content: 50 ppm)*

Industrial samples taken at different times during production of heats—before calcium treatment, shortly after calcium treatment, and long after Ca treatment (tundish and mold samples)—were examined for the presence of intermediate reaction products. The inclusion compositions in the industrial samples were similar to those observed in experimental samples: alumina before calcium treatment (occasionally some calcium and sulfur were also found which could have resulted from impurities in the alloys added); then intermediate reaction products shortly after calcium treatment (CaS in contact with unmodified alumina; Figure 12); and finally liquid calcium aluminate (modified oxide inclusions) in samples taken longer after Ca addition (Figure 13).

The distributions of inclusion compositions (Figure 14) similarly show the shift in inclusion compositions, from a combination of CaS with unmodified alumina in the ladle shortly after calcium treatment to well-modified (mostly liquid) calcium aluminates—containing less sulfur—in the mold. This is also illustrated by the average inclusion compositions (Figure 15): The CaS content shows a maximum in the sample taken just after calcium treatment and is lower in samples taken later, when the inclusions had become more modified.

III. MODIFICATION MECHANISM: EFFECT OF SULFUR CONTENT OF STEEL

The laboratory results suggest a significant difference in modification mechanism for low-sulfur and higher sulfur steels. Based on the results (and recognizing the limits imposed by the presence of undetected inclusions in the steel samples) these differences are identified as follows:

1. In low-sulfur steels, the main calcium reaction product after injection is CaO, whereas the main product is CaS in higher sulfur steels; in general, CaO is not observed as a reaction product in the higher sulfur steels.
2. In samples taken from the higher sulfur steels shortly after calcium injection, CaS is nearly always found to be associated with alumina inclusions, suggesting that the alumina–steel interface is a preferred site for nucleation of CaS.
3. The CaO particles that form in the low-sulfur steel seem not to nucleate on alumina inclusions; the detected CaO inclusions are discrete particles not associated with alumina.
4. The observed changes (with time) in inclusion composition in higher sulfur steels is consistent with CaS reaction with alumina to form calcium aluminate (perhaps via dissolved Ca in the steel as intermediate), rejecting aluminum and sulfur to the steel.
5. For low-sulfur steels, modification might occur by direct reaction between CaO and Al_2O_3. No examples of CaO in contact with alumina or partially modified calcium aluminates could be found in the low-sulfur steels, in contrast with the high frequency of CaS-alumina inclusions observed in the higher sulfur steels shortly after the calcium addition. This finding is in line with the conclusions from previous work on reaction between CaO and Al_2O_3[12]: Those results indicated that at 1873 K (1600 °C) the rate of reaction is limited by the interfacial reaction between alumina and calcium aluminate liquid, and that the rate at which alumina is consumed (the rate of advance of the reaction front) is approximately 20 μm/s.[12] Micron-sized inclusions such as those found in these steels should hence complete reaction within a fraction of a second once contact between CaO and Al_2O_3 has been achieved. As with the case of modification by CaS, there is a possibility of dissolved calcium acting as a reaction intermediate, but the available results do not allow this to be tested.

The steel composition (sulfur concentration) at which the transition occurs from CaO as the main intermediate

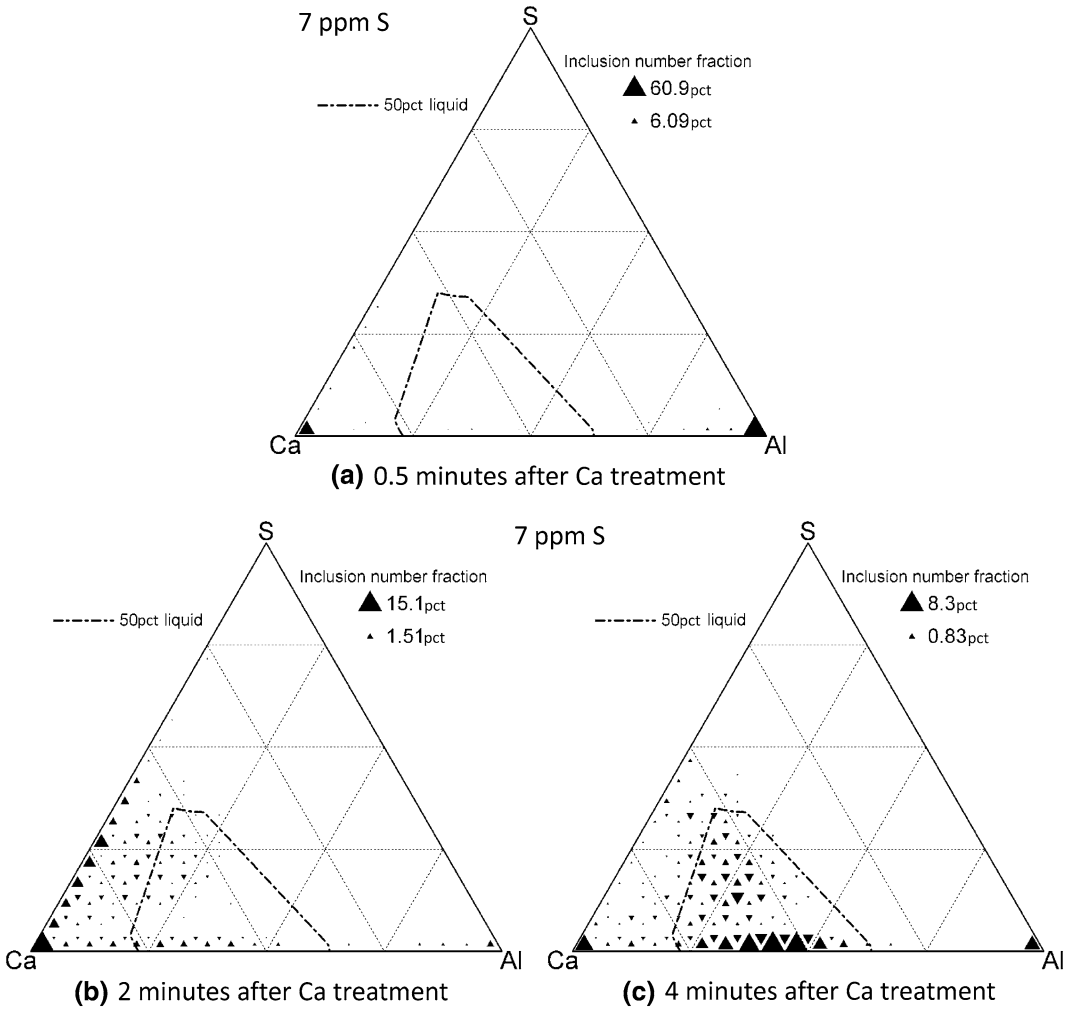

Fig. 4—Distributions of inclusion compositions (on ternary Ca-Al-S diagram; mole fractions), shown as proportional symbol plots. Inclusions in samples collected from heat A (7 ppm S) at various times after calcium treatment (approximately 900 inclusions each).

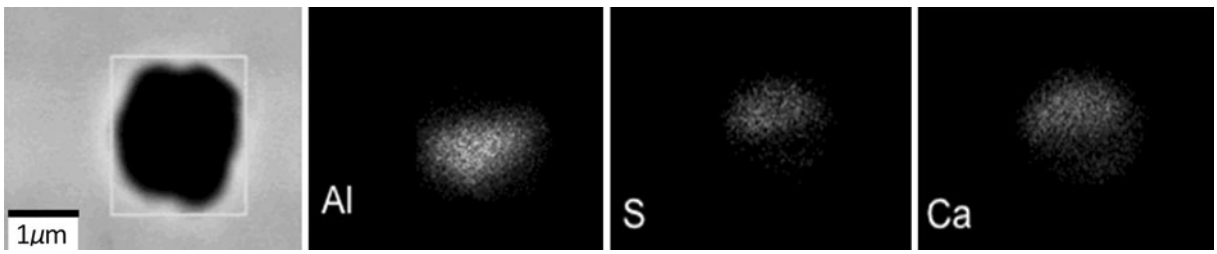

Fig. 5—Element maps (scanning electron microscopy/EDX) showing transient CaS adhering to unmodified Al_2O_3; the image at left is a back-scattered electron image of the inclusion. (heat C; sample collected 2 min after calcium treatment.).

reaction product (in low-sulfur steels) to CaS in higher sulfur steels is expected to be affected by differences in the nucleation behavior of CaO (nucleation sites unknown) and CaS (main nucleation sites apparently alumina–steel interfaces). Competition between oxygen and sulfur for available calcium—whether at the surface of calcium vapor bubbles, or dissolved in the steel—would also affect this transition. Currently, it is not possible to quantify these effects fully, but the relative extents of sulfur and oxygen segregation to the interface between liquid steel and gas (such as calcium vapor) can be estimated using literature data on surface segregation.[13] Figure 16 shows the calculated surface coverages of liquid steel by sulfur and oxygen, using segregation constants based on the effect of oxygen and sulfur on nitrogen–steel reaction kinetics. The segregation constants are 300 for oxygen and 130 for sulfur (for oxygen and sulfur bulk concentrations in

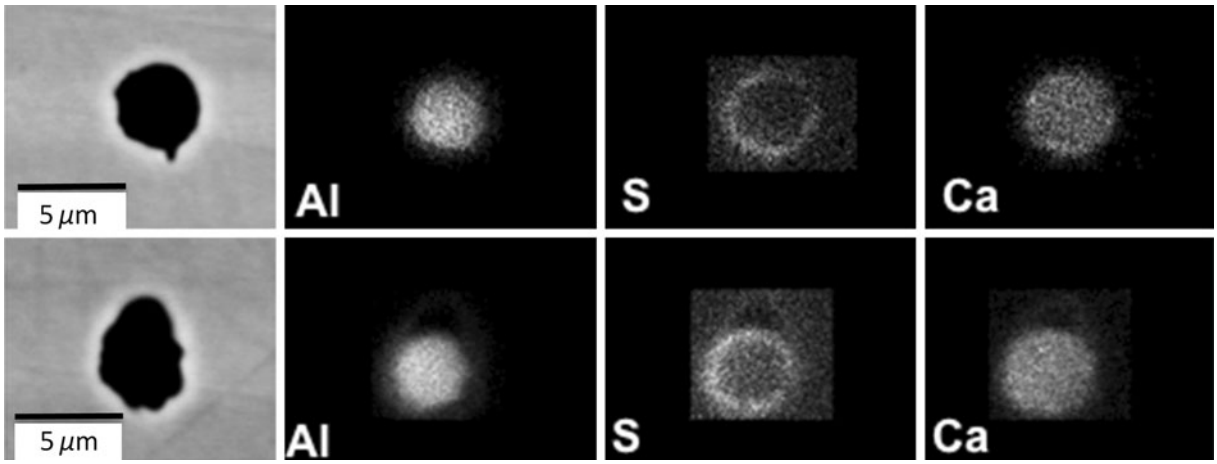

Fig. 6—Inclusions (backscattered electron images at left) with their EDX element maps in sample collected 4 min after calcium treatment (heat C).

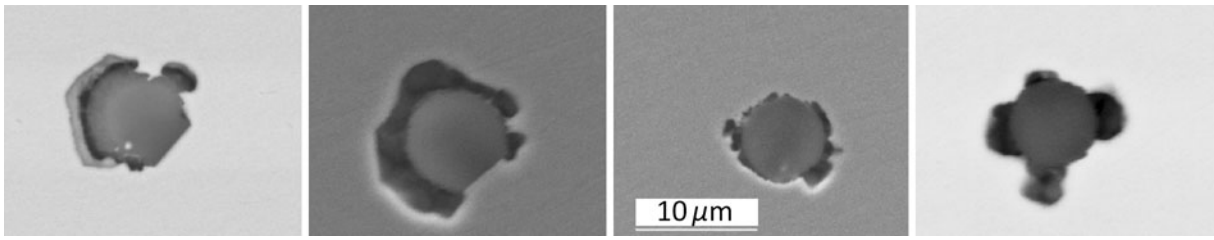

Fig. 7—Inclusions after calcium treatment, showing voids around the inclusions.

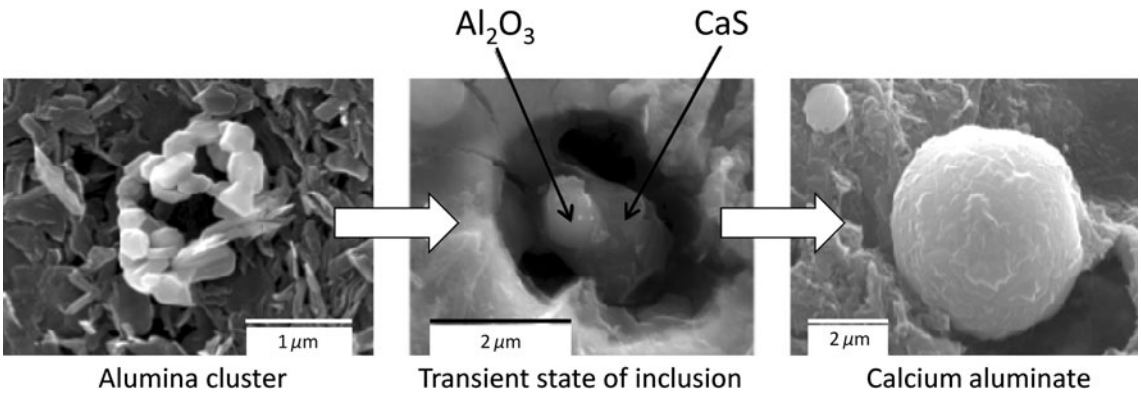

Fig. 8—Modification route of modification of alumina inclusions by calcium, as illustrated by inclusions exposed by bromine-methanol solution (etching of the steel surface in the case of the central image and full dissolution for the other two).

mass percent).[13] The figure is for steel at 1873 K (1600 °C) with a dissolved oxygen activity of 3 ppm (Henrian activity, mass basis) and variable sulfur; it shows that oxygen is the main species segregated to the steel–gas interface for steels containing less than 7 ppm S (and sulfur is the dominant species for steels with more than 7 ppm S). The ratio of surface coverages of oxygen and sulfur is approximately the same as the molar concentrations of these species in the steel (because the product of the mass-based segregation constant and Henrian activity coefficient of oxygen is approximately twice that of sulfur, whereas the molar mass of oxygen is half that of sulfur). Because the transition from oxygen to sulfur as the dominant surface and bulk species occurs at a low sulfur level (7 ppm S), CaS is expected to be the main calcium reaction product in industrially produced steels, which generally contain significantly more sulfur than this.

IV. SUMMARY AND CONCLUSIONS

The mechanism of alumina inclusion modification was investigated by studying inclusion evolution after calcium treatment, for heats with different sulfur contents. Heats containing 40 ppm or more sulfur showed formation of

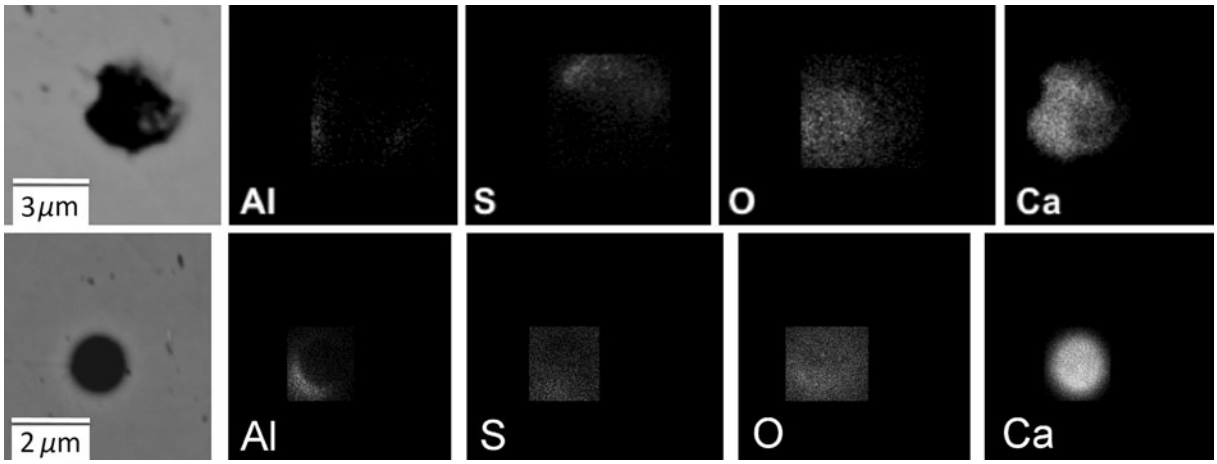

Fig. 9—Examples of inclusions (with element maps) observed in the sample collected 30 s after calcium treatment of the low-sulfur heat (heat A: 7 ppm S).

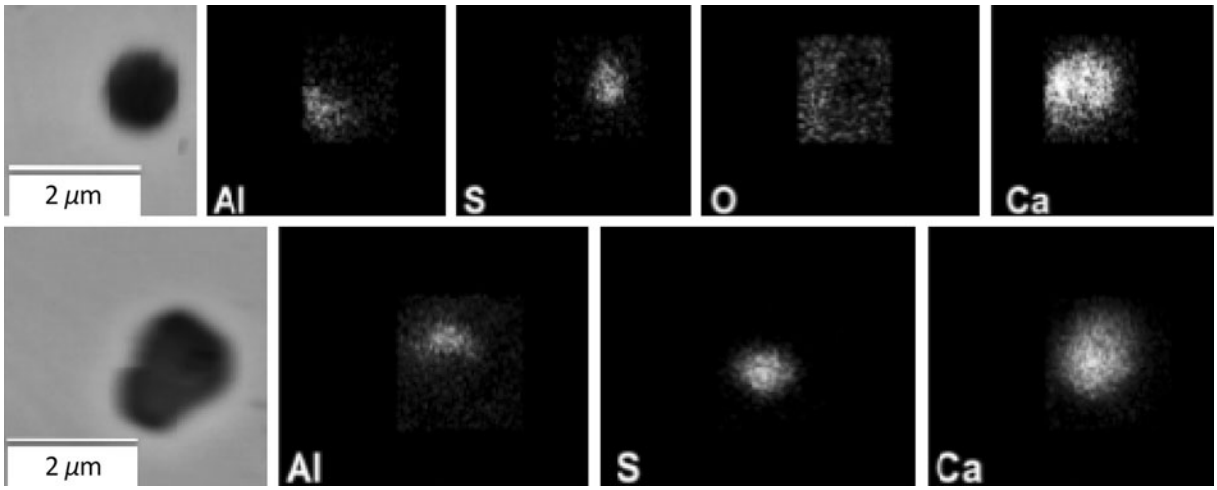

Fig. 10—Examples of inclusions (with element maps) observed in the sample collected 2 minutes after calcium treatment of the low-sulfur heat (heat A: 7 ppm S).

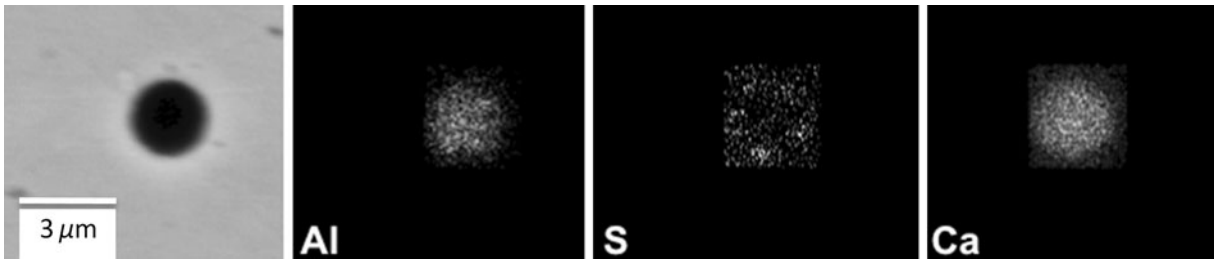

Fig. 11—Example of inclusion (with element maps) observed in the sample collected 4 min after calcium treatment of the low-sulfur heat (heat A: 7 ppm S).

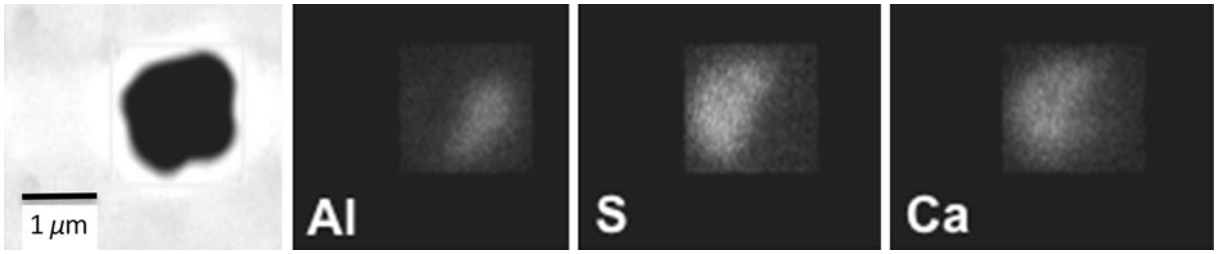

Fig. 12—Transient state in industrial sample: CaS in contact with alumina (sample collected shortly after calcium treatment—ladle sample).

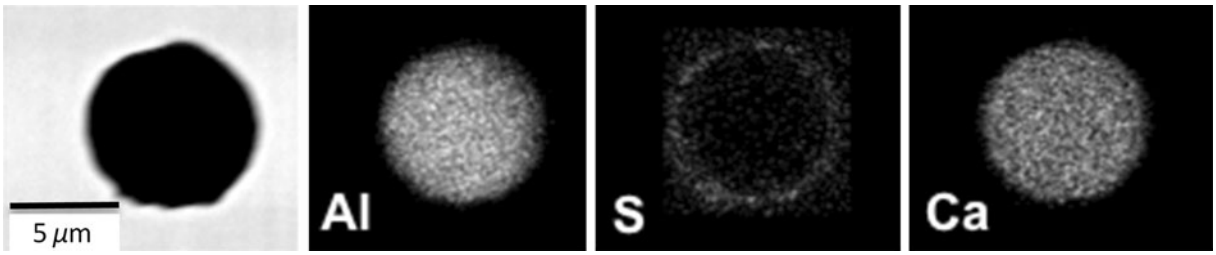

Fig. 13—Fully modified calcium aluminate (liquid at casting temperature) as observed in industrial sample (sample collected long after calcium treatment—mold sample).

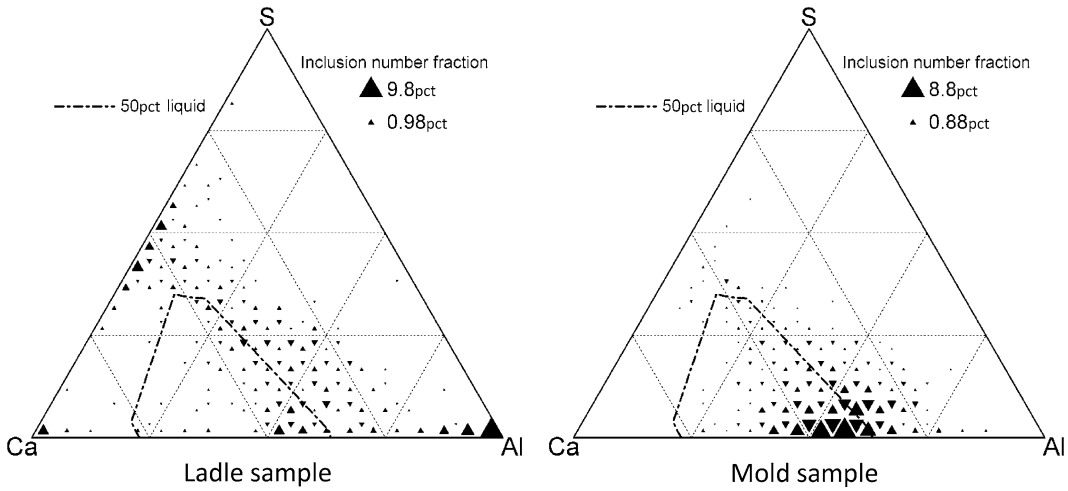

Fig. 14—Distributions of inclusion compositions (on ternary Ca-Al-S diagram; mole fractions), shown as proportional symbol plots. Sample collected from an industrial heat, in the ladle after calcium treatment, and in the mold (ladle—550 inclusions; mold—1000 inclusions).

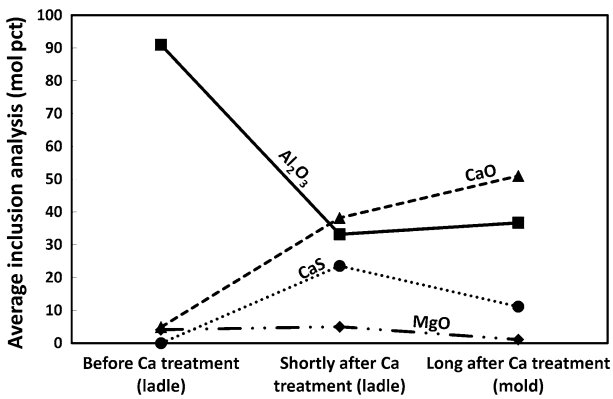

Fig. 15—Number-averaged inclusion analyses in samples taken from industrial heat before Ca treatment, just after Ca treatment, and long after Ca treatment.

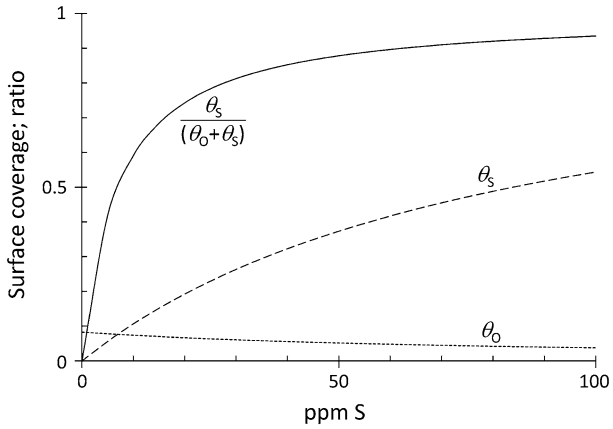

Fig. 16—Calculated coverage of the steel-gas interface by oxygen (θo) and sulfur (θs), for liquid steel at 1873 K (1600 °C) containing O with a Henrian activity of 3 ppm (by mass) and variable sulfur, calculated using the segregation constants $K_O = 300$ and $K_S = 130$.[13] The ratio of surface coverages ($\theta s/[\theta o + \theta s]$) is also shown.

transient CaS, which was consumed as time progressed, causing modification of alumina inclusions. Increased sulfur contents (in the range 40 ppm to 100 ppm) had little effect on the extent of modification of alumina. Industrial heats showed similar evolution of inclusion composition, with CaS as an intermediate reaction product. In low-sulfur laboratory heats (7 ppm S), small CaO inclusions formed after calcium treatment, followed by some CaS formation; both CaO and CaS behaved as transient phases and reacted to modify alumina. Of all the laboratory heats, the alumina inclusions in the low-sulfur heats were best modified by calcium, significantly better than in the higher sulfur heats.

ACKNOWLEDGMENT

Support of this work by the industrial members of the Center for Iron and Steelmaking Research is gratefully acknowledged.

REFERENCES

1. D. Lu, G.A. Irons, and W.K. Lu: *Proc. First International Calcium treatment Symposium*, The Institute of Metals, London, UK, 1988, pp. 23–30.
2. Y. Higuchi, M. Numata, S. Fukagawa, and K. Shinme: *ISIJ Int.*, 1996, vol. 36, pp. S151–S154.
3. W. Tiekink, B. Santillana, R. Boom, R. Kooter, F. Mensonides, and B. Deo: *Iron Steel Technol.*, 2008, vol. 5 (9), pp. 185–95.
4. N. Verma, M. Lind, P.C. Pistorius, R.J. Fruehan, and M. Potter: *Iron Steel Technol.*, 2010, vol. 7 (7), pp. 189–97.
5. C.W. Bale, P. Chartrand, S.A. Degterov, G. Eriksson, K. Hack, R. Ben Mahfoud, J. Melançon, A.D. Pelton, and S. Petersen: *CALPHAD: Comput. Coupling Phase Diagrams Thermochem.*, 2002, vol. 26, pp. 189–228.
6. J.C. Russ: *Practical Stereology*, Plenum Press, New York, NY, 1986, p. 35.
7. W.M. Haynes, ed.: *CRC Handbook of Chemistry and Physics*, 91st ed., CRC Press, Cleveland, OH, 2010, pp. 4-45-56.
8. A. Altay, C.B. Carter, P. Rulis, W.Y. Ching, I. Arslan, and M.A. Gülgün: *J. Solid State Chem.*, 2010, vol. 183, pp. 1776–84.
9. W. Tiekink, R. Boertje, R. Boom, R. Kooter, and B. Deo: *ISSTech 2003 Conf. Proc*, Iron and Steel Society, Warrendale, PA, 2003, pp. 157–64.
10. E.T. Turkdogan: *Arch. Eisenhuettenwes.*, 1983, vol. 54, pp. 1–10.
11. G. Wilde and J.H. Perepezko: *Mater. Sci. Eng. A*, 2000, vol. A283, pp. 25–37.
12. M. Lind and H. Holappa: *Metall. Mater. Trans. B*, 2010, vol. 41B, pp. 359–66.
13. G.R. Belton: *Metall. Trans. B*, 1993, vol. 24B, pp. 241–58.